



Space Technology 5 measurements of auroral field-aligned current sheet motion

Y. Wang,^{1,2} G. Le,² J. A. Slavin,² S. A. Boardsen,^{1,2} and R. J. Strangeway³

Received 11 September 2008; revised 8 December 2008; accepted 11 December 2008; published 30 January 2009.

[1] During the 90-day Space Technology 5 (ST-5) mission, a total of 2535 auroral field-aligned current (FAC) signatures were identified. Of these 1030 were suitable to be modeled as semi-infinite current sheets aligned with L-shells and moving with constant speed in the north or south directions (hereafter called FAC speed). FAC speeds were found to range from -1 to 1 km/s with larger mean magnitude during intervals of higher geomagnetic activity. At ST-5 altitudes, ~ 300 to 4500 km, the median relative errors in FAC thickness and current density, when stationary FAC is assumed, are 4%. When the ST-5 FAC speed determinations are extrapolated along the IGRF-10 magnetic field lines, these errors increase to 23% and 24% at $4 R_E$, and 65% and 124% at $8 R_E$, respectively. **Citation:** Wang, Y., G. Le, J. A. Slavin, S. A. Boardsen, and R. J. Strangeway (2009), Space Technology 5 measurements of auroral field-aligned current sheet motion, *Geophys. Res. Lett.*, *36*, L02105, doi:10.1029/2008GL035986.

1. Introduction

[2] Field-aligned currents (FACs), also called the Birkeland currents, flow into and out of the ionosphere along magnetic field lines. They are the dominant process responsible for transporting energy between the magnetosphere and the ionosphere. FACs with magnitudes of order 10^6 A also heat the upper atmosphere and result in increased drag on low-altitude satellites [Suzuki *et al.*, 1985]. Thus, FACs are important for global magnetosphere-ionosphere dynamics and space weather prediction.

[3] Since their discovery [Zmuda *et al.*, 1966], many studies have been dedicated to the characterization of FACs [e.g., Iijima and Potemra, 1976, 1978; Ishii *et al.*, 1992]. Because FACs are caused by pressure gradients and Maxwell stresses generated in some dynamic regions of the magnetosphere, e.g. the magnetopause and the plasma sheet, they often move in response to changes in magnetospheric configuration. For example, the FAC boundary motions have been found to depend on the direction and intensity of the interplanetary magnetic field (IMF) [Iijima and Potemra, 1978; Fujii *et al.*, 1992; Anderson *et al.*, 2002; Wang *et al.*, 2006].

[4] To unambiguously measure temporal and spatial FAC dynamics, observations from multiple spacecraft are

needed. Kelly *et al.* [1986] calculated the in situ FAC speeds in the current sheet normal direction of 28 FACs using mid- and high-altitude ISEE 1 and 2 magnetic field observations which, when mapped down to the ionosphere, ranged from 50 to 200 m/s [Chun and Russell, 1991]. Lynch *et al.* [1999] used Auroral Turbulence II sounding rocket three-point measurements on 11 February 1997 and found a nightside FAC proper motion speed of 550 m/s northward at less than 500 km altitude. Kistler *et al.* [2002] used Cluster/CIS observations during its perigee midnight auroral zone pass on 23 February 2001 and obtained a speed of ~ 7 km/s for the bulk of ion outflow structures moving equatorward, which corresponds to a velocity of 0.7 km/s at ionosphere. Bosqued *et al.* [2005] studied multi-spacecraft Cluster observations of a northern cusp crossing during a period of high solar wind dynamic pressure and strongly duskward IMF, and found FAC moving predominantly westward with a speed up to ~ 20 km/s at Cluster and ~ 4 km/s when mapped to the ionosphere.

[5] Discrepancies between FAC current densities derived from simultaneous multi-point curlometer calculations compared to those derived from single-point measurements assuming stationary FAC have also been noted. For example, Zheng *et al.* [2003] studied the magnetic field observations from Enstrophy sounding rocket mission with four Free-Flying Magnetometers (FFMs) below ~ 1000 km altitude at the poleward edge of a pre-midnight auroral arc. They found significant differences between the results of the multi-point curlometer calculation of the field-aligned current, and that inferred from any of the single-point observations. They believed that the difference could be caused by the motion of the current structure, which was confirmed by the rapid motion seen in visible auroral structures with in situ current sheet speed from 0.45 km/s to 2.90 km/s between each pair of FFMs.

[6] With the data from the three ST-5 spacecraft, in situ FAC observations with varying ranges in spatial and temporal separations at low altitudes provide an unprecedented opportunity to advance our understanding of FAC structure and dynamics [Slavin *et al.*, 2008]. These data allow, for the first time, the separation of temporal and spatial variations in FAC perturbations measured in low Earth orbit (LEO) on temporal scales from ~ 10 sec to ~ 10 min and spatial scales from ~ 50 to ~ 5000 km. The ST-5 FAC data set also makes it possible to systematically evaluate the effects of FAC sheet speed on FAC thickness and current density calculations, which was not possible due to the limited number of in situ multi-spacecraft FAC observations from earlier missions.

[7] In this paper, first we describe the data and method used to obtain FAC speed. Then we determine the distribution of FAC ionospheric footprint speed and examine its

¹Goddard Earth Sciences and Technology Center, University of Maryland Baltimore County, Baltimore, Maryland, USA.

²Heliophysics Science Division, NASA Goddard Space Flight Center, Greenbelt, Maryland, USA.

³Institute of Geophysics and Planetary Physics, University of California, Los Angeles, California, USA.

dependence on geomagnetic activity. Finally, we investigate the influence of FAC speed on FAC thickness and current density calculations at LEO and higher altitudes to characterize the uncertainties introduced by the customary assumption of stationary FAC.

2. Data Analysis

[8] The three-spacecraft ST-5 constellation was launched on 22 March 2006 into a single elliptical Sun synchronous orbit with altitude ranging from 300 km to 4500 km and an orbital inclination of 105.6° [Slavin *et al.*, 2008]. After deployment, the micro-satellites were positioned in a “string of pearls” constellation with orbital period of 136 minutes and spin period near 3 seconds. The lead, middle, and trailing ST-5 satellites are called SC155, SC094, and SC224, respectively. Each spacecraft carried a fluxgate magnetometer with 0.1 nT and 1 nT resolution in their low- and high-field ranges, respectively. The ST-5 mission lasted 90 days as planned and was decommissioned on 21 June 2006. For a more comprehensive overview of the ST-5 mission, please refer to Slavin *et al.* [2008].

[9] In this study, we used the 1-s averaged magnetic field observations for the whole ST-5 mission. To identify FACs, we first subtracted the background magnetic field, using IGRF-10 [Macmillan and Maus, 2005], from ST-5 magnetic field observations to separate the small perturbations caused by FAC from the main field. Local Geomagnetic (LGM) coordinates were used for our analysis. In this coordinate system, \hat{z} is along the local IGRF-10 magnetic field, \hat{y} is the cross product of \hat{z} and a unit vector in the geomagnetic east direction, and \hat{x} completes the right-handed orthogonal coordinate system. Because the ST-5 spacecraft formed a 1-D array we still must assume that the FACs are semi-infinite sheets aligned with the LGM xz plane. Since currents flow along field lines in the LGM z direction, we expect the maximum disturbances of the residual magnetic field by FAC to be along the LGM x direction. Instead of using different LGM transformations at different data points as many earlier studies did [e.g., Stauning *et al.*, 2001; Wang *et al.*, 2006], we used a common LGM transformation matrix for the magnetic field observations from all three ST-5 spacecraft for each FAC signature to allow inter-spacecraft comparison.

[10] The middle ST-5 spacecraft, SC094, was used to identify FAC events. FACs have a clear bell-shaped or reverse bell-shaped structure in the residual magnetic field in the LGM x direction, $\delta B_{x|lgm}$, superimposed on the background which corresponds to a pair of upward and downward currents [Slavin *et al.*, 2008]. A total of 2535 FAC signatures were identified in the ST-5 mission data set. For each FAC signature, we identified the times when SC094 encountered the start and end of the FAC signature, then obtained its central time, $T_{c,094}$, and central location, $\mathbf{R}_{c,094}$. We then applied the common LGM transformation matrix at $\mathbf{R}_{c,094}$ to SC155 and SC224 magnetic field measurements.

[11] The observed current sheet motion in its normal direction, hereafter called current sheet motion, can be either due to the drift of the source region or $\mathbf{E} \times \mathbf{B}$ drift of the current carriers anywhere along the field-aligned current precipitation path [e.g., Lynch *et al.*, 1999]. Here, we followed Chun and Russell [1991] in assuming that

current sheet motion can be well approximated as the transfer of entire current sheet structure to new field lines. Note here that FAC speed used in this study is the apparent current sheet motion speed in its normal direction instead of the current carrier speed. To calculate FAC speed for each FAC signature, we time shifted the SC155 and SC224 $\delta B_{x|lgm}$ against the SC094 $\delta B_{x|lgm}$ and found the temporal offset that produced the largest cross-correlation coefficient. A similar method was used by Kelly *et al.* [1986] to calculate FAC speed with ISEE 1 and 2 observations. Below we assume for illustrative purpose that the SC094-SC155 pair has the largest cross-correlation coefficient. The SC155 FAC central time, $T_{c,155}$, can be obtained from $T_{c,094}$ and the timeshift between SC094 and SC155 based on the above cross-correlation analysis. SC155 FAC central location at $T_{c,155}$, $\mathbf{R}_{c,155}$, can further be obtained. Finally, we can calculate FAC speed, V^{FAC} , using:

$$V^{FAC} = \left(\frac{y_{c,094} - y_{c,155}}{T_{c,094} - T_{c,155}} \right), \quad (1)$$

here $y_{c,094}$ and $y_{c,155}$ are the y components of $\mathbf{R}_{c,094}$ and $\mathbf{R}_{c,155}$, respectively, in current sheet normal direction.

[12] To ensure the quality of our statistics, the following six rejection criteria were used on the initial 2535 FACs to screen out events that were not consistent with our moving current sheet model and/or had excessive errors in V^{FAC} . (i) Eigenvalues from the Minimum Variance Analysis (MVA) [Sonnerup and Scheible, 1998] correspond to the variances in the field components in the minimum, medium, and maximum variance directions. They were computed for each SC094 FAC segment to make sure that the angle between the FAC maximum field variation direction, corresponding to the maximum MVA eigenvalue, and the LGM x axis is less than 30° . About 28% of our initial FACs are outside of this range, which could be due to current sheets whose orientation was significantly different from the LGM xz plane, or edge effects associated with the spacecraft encountering finite current sheets [Fung and Hoffman, 1992]. (ii) We excluded the FACs with the ratios of the maximum to intermediate MVA eigenvalues less than 10/3 ($\sim 7\%$ of all our initial FACs) to make sure that the variations along the maximum variance direction are much more significant than those in the other directions. (iii) Since we used a constant LGM transformation matrix on the magnetic field data from all three ST-5 spacecraft for each FAC, we placed another criterion to ensure that the transformation matrix was valid throughout the entire FAC interval. Otherwise, the resulting $\delta B_{x|lgm}$ values at the boundaries can be very different from the actual ones from using local LGM transformation matrix. To achieve this, we excluded all the FAC signatures with the maximum Euler angles between the central and the two boundary LGM transformation matrixes larger than 10° ($\sim 19\%$ of the initial FACs). (iv) Those FACs with the maximum cross-correlation coefficients between the chosen spacecraft pairs smaller than 0.9 ($\sim 6\%$ of the initial FACs) were also excluded. This restricted our FAC database to the ones whose properties did not change significantly between the chosen ST-5 pairs. (v) The attack angle of each FAC encounter is defined as the angle between current sheet normal direction (the LGM y direction) and spacecraft

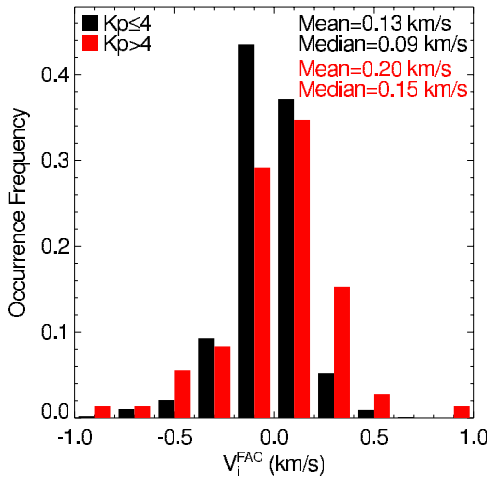


Figure 1. The occurrence frequency of FAC ionospheric footprint speed, V_i^{FAC} , for $K_p \leq 4$ (958 FACs) and $K_p > 4$ (72 FACs), with positive/negative speed pointing approximately equatorward/poleward.

trajectory. In this study, we further removed the cases with attack angles larger than 60° ($\sim 18\%$ of the initial FACs) to avoid ST-5 skimming along current sheets, which makes the determination of FAC speed and current density unreliable. (vi) The time resolution of the data used in this study, 1 second, is usually much smaller than, but can also be comparable to, the FAC central time difference in equation (1) (~ 10 seconds to minutes). Meanwhile, the inter-spacecraft position error of 1 km [Slavin *et al.*, 2008] can in many occasions be comparable to the separation of the observed FAC locations in equation (1). To ensure the accuracy of FAC speed calculations, we excluded those FACs with speed errors, derived using standard error estimates from uncorrelated measurements, larger than 0.1 km/s ($\sim 13\%$ of the initial FACs). The above six criteria reduced the total number of FACs to 1030 that can be accurately modeled using our assumption of sheet-like FACs in the LGM xz plane with constant FAC speed. This subset was subjected to our full analysis.

[13] FAC speed can be mapped along IGRF-10 field lines to the ionosphere and higher altitudes to study its dependence on geomagnetic activity and/or its effects on FAC thickness and current density calculations. Such mapping

removes spacecraft orbit altitude biases and puts all the FACs on the same ground for comparison. Based on magnetic flux conservation within a flux tube which connects ST-5 to any position along the flux tube, we have $|\mathbf{B}_{ST-5}| \cdot \delta y_{ST-5}^{LGM} \cdot \delta x_{ST-5}^{LGM} = |\mathbf{B}_{map}| \cdot \delta y_{map}^{LGM} \cdot \delta x_{map}^{LGM}$. Since the field line is mainly confined to the meridional plane, for the two field lines separated by $\delta\phi$ in magnetic longitude, we have $\delta x_{ST-5}^{LGM} = \delta\phi \rho_{ST-5}$ and $\delta x_{map}^{LGM} = \delta\phi \rho_{map}$, here ρ_{ST-5} and ρ_{map} are the distance from the Earth dipole axis. Also considering $\delta y_{ST-5}^{LGM} = V^{FAC} \delta t$ and $\delta y_{map}^{LGM} = V_{map}^{FAC} \cdot \delta t$ (here δt is a very small time interval), we have:

$$V_{map}^{FAC} = V^{FAC} \frac{|B_{ST-5}| \rho_{ST-5}}{|B_{map}| \rho_{map}}. \quad (2)$$

For FAC ionospheric footprint speed at 100 km altitude parallel to the Earth surface, V_i^{FAC} , we have $V_i^{FAC} = V_{map}^{FAC} |\cos\theta|$, where θ is the angle between the IGRF-10 magnetic field and the Earth radial direction at the ionospheric footprint.

3. Results

[14] Figure 1 shows the occurrence frequency of V_i^{FAC} for low/high geomagnetic activity ($K_p \leq 4/K_p > 4$) ranging from -1 to 1 km/s with the majority ($\sim 97\%$) of FACs having $|V_i^{FAC}|$ smaller than 0.5 km/s. We see generally enhanced $|V_i^{FAC}|$ during high geomagnetic activity (mean 0.20 km/s and median 0.15 km/s) than during low geomagnetic activity (mean 0.13 km/s and median 0.09 km/s) for both poleward (negative V_i^{FAC}) and equatorward (positive V_i^{FAC}) motion.

[15] The ratio of FAC speed to spacecraft speed along the LGM y direction, V^{FAC}/V_y^{SC} , is linearly related to the errors in FAC thickness and current density calculations if stationary FACs are assumed [Slavin *et al.*, 2008]. At higher altitude, the speed of Earth circling satellite, under Earth's gravitational field, is usually smaller and FAC speed is usually larger from equation (2). As a result, the uncertainties from FAC speed will be larger than those at LEO. Figure 2 shows the occurrence frequency of $|V^{FAC}/V_y^{SC}|$ at ST-5 (Figure 2 (left)), as well as mapped to $R = 4 R_E$ (Figure 2 (middle)) and $R = 8 R_E$ (Figure 2 (right)), along IGRF-10 field lines. Here the speeds of spacecraft on circular orbits around the Earth at $R = 4 R_E$, 3.95 km/s,

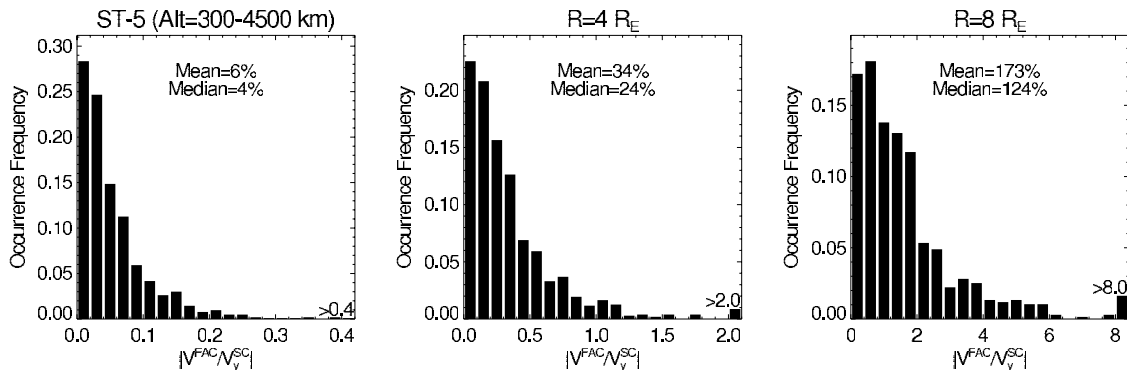


Figure 2. The occurrence frequency of the ratios between FAC and spacecraft speed magnitude at (left) ST-5 position, as well as (middle) mapped to $R = 4 R_E$ and (right) $R = 8 R_E$ along IGRF-10 field lines. Circular orbit spacecraft speeds are used for the mapped cases assuming they are along current sheet normal directions.

and $R = 8 R_E$, 2.79 km/s, are used for the mapped cases assuming spacecraft orbit perpendicular to current sheet, which is a reasonable assumption close to the dawn-dusk meridional plane where ST-5 orbit resided and at high latitudes ($>45^\circ$) where all our ST-5 FACs were identified. This is the simplest scenario to estimate FAC thickness and current density uncertainties related to FAC speed. For the ST-5 case in Figure 2 (left), the $|V^{FAC}/V_y^{SC}|$ ratio ranges from 0% to more than 40%, with $\sim 15\%$ of the ratios larger than 10%. The mean and median ratios are 6% and 4%, respectively. For the $4 R_E$ mapped case in Figure 2 (middle), the $|V^{FAC}/V_y^{SC}|$ ratio is as high as 2, with 5% greater than 1. The mean and median ratios are 34% and 24%, respectively. For the $8 R_E$ mapped case in Figure 2 (right), the $|V^{FAC}/V_y^{SC}|$ ratio shows values as large as 8 with $\sim 57\%$ of the ratios larger than 1. The mean and median ratios are 173% and 124%, respectively. Considering that spacecraft orbits are not generally perpendicular to current sheets, as well as the distortion of current sheets and large-scale motion of plasmas at high altitudes, the uncertainty at $R = 4$ and $8 R_E$ can be even larger.

4. Discussion and Conclusions

[16] ST-5 data set allows us to calculate LEO FAC speeds on temporal scales from ~ 10 sec to ~ 10 min and spatial scales from ~ 50 to ~ 5000 km that have not been possible from previous in situ observations [Slavin *et al.*, 2008]. FAC speed is found to be associated with geomagnetic activity with generally faster/slower motion during stronger/weaker geomagnetic activity, consistent with earlier observations [e.g., Fujii *et al.*, 1992; Anderson *et al.*, 2002; Wang *et al.*, 2006]. However, even during periods of intense geomagnetic activity, a significant number of FACs with low speeds were observed, and, vice versa, during low geomagnetic activity. The FAC ionospheric footprint speeds of 50 to 200 m/s obtained by Chun and Russell [1991] are in good agreement with the ST-5 FAC results presented here. However, our study has also revealed large number of FACs with ionospheric footprint speeds as large as 1 km/s.

[17] Knowledge of FAC speed can also be used to assess the accuracy of single spacecraft calculations of FAC properties, including current sheet thickness and current density. The relative errors of FAC thickness and current density, assuming stationary FAC, are:

$$E_{thickness} = \frac{\left| V_y^{SC} \Delta t - (V_y^{SC} - V^{FAC}) \Delta t \right|}{\left| (V_y^{SC} - V^{FAC}) \Delta t \right|} = \frac{\left| \frac{V^{FAC}}{V_y^{SC}} \right|}{\left| 1 - \frac{V^{FAC}}{V_y^{SC}} \right|}, \quad (3)$$

$$E_{current\ density} = \frac{\left| -\frac{1}{\mu_0} \frac{1}{V_y^{SC}} \frac{\partial B_{xlgm}}{\partial t} - \left(-\frac{1}{\mu_0} \frac{1}{V_y^{SC} - V^{FAC}} \frac{\partial B_{xlgm}}{\partial t} \right) \right|}{\left| -\frac{1}{\mu_0} \frac{1}{V_y^{SC} - V^{FAC}} \frac{\partial B_{xlgm}}{\partial t} \right|} = \frac{\left| \frac{V^{FAC}}{V_y^{SC}} \right|}{\left| \frac{V_y^{SC}}{V_y^{SC} - V^{FAC}} \right|}, \quad (4)$$

here Δt is the time taken for the spacecraft to traverse the current sheet. The median values for both $E_{thickness}$ and $E_{current\ density}$ of the 1030 ST-5 FACs are 4%. FAC speed is expected to have more significant impact on the calculations at higher altitudes since spacecraft speed decreases and FAC speed increases with increasing altitude. This is confirmed with increased median $E_{thickness}$ of 23% and $E_{current\ density}$ of 24% at $R = 4 R_E$, and 65% for $E_{thickness}$ and 124% for $E_{current\ density}$ at $R = 8 R_E$. It is concluded that estimates of Birkeland current densities and thickness using traversals of the currents by single satellites are generally reliable in LEO, with errors typically smaller than 10%. The extrapolated uncertainties in FAC thickness and current density at higher altitudes urge caution in the use of single satellite observations to determine FAC properties especially during periods of high geomagnetic activity. For comparison, Kelly *et al.* [1986] studied 31 January 1978 ISEE 1 and 2 FAC observations at close to $R = 4 R_E$ and obtained an FAC speed of -2.89 km/s and a spacecraft speed of 1.36 km/s, which lead to $E_{thickness}$ and $E_{current\ density}$ of 68% and 213%, respectively, when stationary FAC is assumed. These errors are larger than our median $E_{thickness}$ and $E_{current\ density}$ at $R = 4 R_E$, but are within our maximum error estimations at this altitude. One should note that our simplified error estimation method is not applicable to ISEE 1 and 2 because their orbits have much lower inclination and greater ellipticity than ST-5.

[18] **Acknowledgments.** We thank NOAA/NGDC for providing the Kp indexes. YW would like to thank M.E. Purucker and M.A. Concha for the very helpful discussions about ST-5 orbit position errors.

References

- Anderson, B. J., K. Takahashi, T. Kamei, C. L. Waters, and B. A. Toth (2002), Birkeland current system key parameters derived from Iridium observations: Method and initial validation results, *J. Geophys. Res.*, *107*(A6), 1079, doi:10.1029/2001JA000080.
- Bosqued, J. M., et al. (2005), Multipoint observations of transient reconnection signatures in the cusp precipitation: A Cluster-IMAGE detailed case study, *J. Geophys. Res.*, *110*, A03219, doi:10.1029/2004JA010621.
- Chun, F. K., and C. T. Russell (1991), The evolution of field-aligned currents as a function of substorm phase, *J. Geophys. Res.*, *96*, 15,801–15,810.
- Fujii, R., H. Fukunishi, S. Kokubun, M. Sugiura, F. Tohyama, H. Hayakawa, K. Tsuruda, and T. Okada (1992), Field-aligned current signatures during the March 13–14, 1989, great magnetic storm, *J. Geophys. Res.*, *97*, 10,703–10,715.
- Fung, S. F., and R. A. Hoffman (1992), Finite geometry effects of field-aligned currents, *J. Geophys. Res.*, *97*, 8569–8579.
- Iijima, T., and T. A. Potemra (1976), Field-aligned currents in the dayside cusp observed by Triad, *J. Geophys. Res.*, *81*, 5971–5979.
- Iijima, T., and T. A. Potemra (1978), Large-scale characteristics of field-aligned currents associated with substorms, *J. Geophys. Res.*, *83*, 599–615.
- Ishii, M., M. Sugiura, T. Iyemori, and J. A. Slavin (1992), Correlation between magnetic and electric field perturbations in the field-aligned current regions deduced from DE 2 observations, *J. Geophys. Res.*, *97*, 13,877–13,887.
- Kelly, T. J., C. T. Russell, R. J. Walker, G. K. Parks, and J. T. Gosling (1986), ISEE 1 and 2 observations of Birkeland currents in the Earth's inner magnetosphere, *J. Geophys. Res.*, *91*, 6945–6958.
- Kistler, L. M., et al. (2002), Motion of auroral ion outflow structures observed with CLUSTER and IMAGE FUV, *J. Geophys. Res.*, *107*(A8), 1186, doi:10.1029/2001JA005075.
- Lynch, K. A., D. Pietrowski, R. B. Torbert, N. Ivchenko, G. Marklund, and F. Prindahl (1999), Multiple-point electron measurements in a nightside auroral arc: Auroral Turbulence II particle observations, *Geophys. Res. Lett.*, *26*, 3361–3364.
- Macmillan, S., and S. Maus (2005), International geomagnetic reference field—The tenth generation, *Earth Planets Space*, *57*, 1135–1140.

- Slavin, J. A., G. Le, R. J. Strangeway, Y. Wang, S. A. Boardsen, M. B. Moldwin, and H. E. Spence (2008), Space Technology 5 multi-point measurements of near-Earth magnetic fields: Initial results, *Geophys. Res. Lett.*, *35*, L02107, doi:10.1029/2007GL031728.
- Sonnerup, B. U. Ö., and M. Scheible (1998), Minimum and maximum variance analysis, in *Analysis Methods for Multi-spacecraft Data*, edited by G. Paschmann and P. W. Daly, *Eur. Space Agency Spec. Publ., ESA SP-449*, pp. 183–220.
- Stauning, P., F. Primdahl, J. Watermann, and O. Rasmussen (2001), IMF B_y -related cusp currents observed from the Ørsted Satellite and from ground, *Geophys. Res. Lett.*, *28*, 99–102.
- Suzuki, A., M. Yanagisawa, and N. Fukushima (1985), Antisunward space current below the MAGSAT level during magnetic storms and its possible connection with partial ring current in the magnetosphere, *J. Geophys. Res.*, *90*, 2465–2471.
- Wang, H., H. Lüher, S.Y. Ma, J. Weygand, R.M. Skoug, and F. Yin (2006), Field-aligned currents observed by CHAMP during the intense 2003 geomagnetic storm events, *Ann. Geophys.*, *24*, 311–324.
- Zheng, Y., K. A. Lynch, M. Boehm, R. Goldstein, H. Javadi, P. Schuck, R. L. Arnoldy, and P. M. Kintner (2003), Multipoint measurements of field-aligned current density in the auroral zone, *J. Geophys. Res.*, *108*(A5), 1217, doi:10.1029/2002JA009450.
- Zmuda, A. J., J. H. Martin, and F. T. Heuring (1966), Transverse magnetic disturbances at 1100 kilometers in the auroral region, *J. Geophys. Res.*, *71*, 5033–5045.
-
- S. A. Boardsen and Y. Wang, Heliophysics Science Division, NASA Goddard Space Flight Center, Mail Stop 674, Greenbelt, MD 20771, USA. (yongli.wang@nasa.gov)
- G. Le, Heliophysics Science Division, NASA Goddard Space Flight Center, Mail Stop 674, Greenbelt, MD 20771, USA.
- J. A. Slavin, Heliophysics Science Division, NASA Goddard Space Flight Center, Mail Stop 670, Greenbelt, MD 20771, USA.
- R. J. Strangeway, Institute of Geophysics and Planetary Physics, University of California, 405 Hilgard Avenue, Los Angeles, CA 90095, USA.